Long-term Late Cretaceous carbon- and oxygen-isotope trends and planktonic foraminiferal turnover: a new record from the southern mid-latitudes

Francesca Falzoni[1*], Maria Rose Petrizzo[1], Leon J. Clarke[2], Kenneth G. MacLeod[3] and Hugh C. Jenkyns[4]

*[1]Francesca Falzoni, Dipartimento di Scienze della Terra "A. Desio", Università degli Studi di Milano, via Mangiagalli 34, 20133 Milano, Italy (*Corresponding author's e-mail: francesca.falzoni@unimi.it).*

[1]Maria Rose Petrizzo, Dipartimento di Scienze della Terra "A. Desio", Università degli Studi di Milano, via Mangiagalli 34, 20133 Milano, Italy (e-mail: mrose.petrizzo@unimi.it).

[2]Leon J. Clarke, School of Science and the Environment, Manchester Metropolitan University, Chester Street, Manchester, M1 5GD, UK (e-mail: l.clarke@mmu.ac.uk).

[3]Kenneth G. MacLeod, Department of Geological Sciences, University of Missouri-Columbia, 101 Geological Sciences Bldg., Columbia, MO 65211, USA (e-mail: MacLeodK@missouri.edu).

[4]Hugh C. Jenkyns, Department of Earth Sciences, University of Oxford, South Parks Road Oxford, OX1 3AN, UK (e-mail: hugh.jenkyns@earth.ox.ac.uk).

Running title: Late Cretaceous stable-isotope trends

ABSTRACT

The ~35 myr-long Late Cretaceous greenhouse climate has been subjected to a number of studies with emphasis on the Cenomanian–Turonian and late Campanian–Maastrichtian intervals. By contrast, far less information is available for the Turonian–early Campanian interval, even though it encompasses the transition out of the extreme warmth of the Cenomanian–Turonian greenhouse climate optimum and includes a ~3 myr-long mid-Coniacian–mid-Santonian interval when planktonic foraminifera underwent a large-scale, but poorly understood, turnover. This study presents ~1350 $\delta^{18}O$ and $\delta^{13}C$ values of well-preserved benthic and planktonic foraminifera and of the <63 μm size fraction from the Exmouth Plateau off Australia (eastern Indian Ocean). These data provide: (i) the most continuous, highly resolved and stratigraphically well-constrained record of long-term trends in Late Cretaceous oxygen- and carbon-isotope ratios from the southern mid-latitudes, and (ii) new information on the paleoecological preferences of planktonic foraminiferal taxa. The results indicate persistent warmth from the early Turonian until the mid-Santonian, cooling from the mid-Santonian through the mid-Campanian, and short-term climatic variability during the late Campanian–Maastrichtian. Moreover, our results suggest the cause of Coniacian–Santonian turnover among planktonic foraminifera may have been the evolution of a temperature/salinity-tolerant genus (*Marginotruncana*) and the cause of the Santonian–early Campanian extinction of *Dicarinella* and *Marginotruncana* may have been surface-ocean cooling and competition with globotruncanids.

INTRODUCTION

45 The Late Cretaceous was characterized by extreme greenhouse climate conditions likely
46 forced by high atmospheric pCO_2 levels (estimated up to 1300 ppmv: Sinninghe Damsté et al.,
47 2008), with maximum warmth likely reached during the Cenomanian–Turonian (Jenkyns et al.,
48 1994; Clarke and Jenkyns, 1999; Voigt et al., 2004; Friedrich et al., 2012), when surface-ocean
49 temperatures reached ~36°C in the tropical and equatorial belts (Forster et al., 2007; Moriya et
50 al., 2007; MacLeod et al., 2013), and equator to high latitude (~70°S) sea-surface temperature
51 gradients could have been reduced to ~5°C (Huber et al., 2002; Linnert et al., 2014). This warm
52 phase was followed by a prolonged cooling trend until the mid-Campanian (Clarke and Jenkyns,
53 1999; Huber et al., 2002; Cramer et al., 2009; Friedrich et al., 2012; Linnert et al., 2014), with
54 lower amplitude cooling and warming episodes during the late Campanian–Maastrichtian (Li and
55 Keller, 1999; Abramovich et al., 2010; Friedrich et al., 2012; Linnert et al., 2014) and regional
56 differences in both surface (MacLeod et al., 2005; Isaza Londoño et al., 2006) and bottom-water
57 trends (Cramer et al., 2009). However, while most studies on Late Cretaceous paleoclimate have
58 been focused on relatively short-duration events (e.g., Cenomanian/Turonian boundary, Oceanic
59 Anoxic Event 2 and the Cretaceous/Paleogene boundary mass extinction), far less information is
60 available for the ~20 myr-long Turonian–Campanian interval.
61 Planktonic foraminifera underwent a ~3 myr-long major turnover during the mid-
62 Coniacian–mid-Santonian (Hart 1999; Premoli Silva and Sliter, 1999), followed by the
63 extinction of all pre-Campanian double-keeled taxa (*Marginotruncana* and *Dicarinella*) within
64 the latest Santonian–earliest Campanian. The cause(s) of these events has/have never been
65 established. This lack of understanding relates to the limited recovery of stratigraphically
66 complete Turonian–early Campanian sediments by DSDP (Deep Sea Drilling Project), ODP
67 (Ocean Drilling Program) and IODP (Integrated Ocean Drilling Program), as well as the

68 generally poor preservation of Turonian–lower Campanian microfossils from outcrop sections,
69 which are dominated by indurated limestones. Low geographic and stratigraphic resolution
70 complicates correlation, whereas diagenetic artifacts associated with relatively poor preservation
71 compromises interpretation of stable-isotope measurements for reconstructing paleoceanographic
72 and paleoclimatic changes (e.g., Pearson et al., 2001; Sexton et al., 2006), species depth
73 preferences (e.g., Ando et al., 2010; Falzoni et al., 2013), and other aspects of paleoecology
74 (opportunism, seasonal preferences, photosymbionts) (e.g., Abramovich et al., 2003; Petrizzo et
75 al., 2008; Falzoni et al., 2014). Further uncertainty concerning the paleoecology (including depth
76 habitats) of Cretaceous planktonic foraminifera has been demonstrated by the results of several
77 studies that found the traditional morphology-based scheme for inferring Cretaceous planktonic
78 foraminiferal paleoecology to be probably incorrect for many taxa (Abramovich et al., 2003;
79 Ando et al., 2010; Falzoni et al., 2013).
80 This study, based on well-preserved planktonic and benthic foraminiferal $\delta^{18}O$ and $\delta^{13}C$
81 values from Exmouth Plateau (ODP Leg 122, Hole 762C, eastern Indian Ocean), provides the
82 most complete, continuous, highly resolved and stratigraphically well-constrained Late
83 Cretaceous record of climatic change and of long-term carbon-isotope trends in the southern
84 mid-latitudes. Oxygen and carbon stable-isotope ratios derived from the <63 μm fine fraction
85 have been plotted to compare the trends for such samples with those shown by foraminifera, in
86 order to evaluate similarities and differences. Moreover, the present study provides new
87 information on the paleoecological preferences of several planktonic foraminiferal taxa for
88 which no stable-isotope ratio data were previously available, thereby providing new information
89 on the timing and causes of Late Cretaceous planktonic foraminiferal turnover.
90

MATERIALS AND METHODS

ODP Hole 762C was cored during Leg 122 on the central Exmouth Plateau, northwestern Australian margin (19°53.24'S; 112°15.24'E; Haq et al., 1990; Fig. 1) and recovered a nearly continuous Berriasian–lower Oligocene sequence. The Upper Cretaceous sequence is almost complete, with two minor hiatuses, one in the lower Santonian (core 67X; Petrizzo, 2000) and the other in the mid-Maastrichtian, within magnetic chron C31N (core 47X; Thibault et al., 2012). The Santonian hiatus is estimated to span less than 700 kyr (Petrizzo, 2000), whereas the Maastrichtian hiatus spans about 500 kyr (Thibault et al., 2012). Upper Cretaceous sediments mainly consist of white to reddish calcareous nannofossil ooze (Haq et al., 1990), with abundant planktonic, and rare benthic foraminifera (Zepeda, 1998; Petrizzo, 2000, 2002). Taxonomic concepts applied in this study for the identification of planktonic and benthic foraminifera follow Robaszynski et al. (1979, 1984), Wonders (1992), Huber and Leckie (2011), Falzoni and Petrizzo (2011), Petrizzo et al. (2011, 2015), Falzoni et al. (2016), the CHRONOS online Mesozoic Planktonic Foraminiferal Taxonomic Dictionary (http://portal.chronos.org), Loeblich and Tappan (1988) and the Ellis and Messina online catalogue (www.micropress.org). We have included in the genus *Heterohelix* sensu latu ("*Heterohelix*") all biserial species that were previously accommodated in this polyphyletic group (e.g., *globulosa*, *moremani*), as is it currently under revision (see Haynes et al., 2015), and species are believed to share almost the same paleoecological preferences (Premoli Silva and Sliter, 1999; Abramovich et al., 2003; Haynes et al., 2015). The biostratigraphic framework applied here follows Haq et al. (1990), Bralower and Siesser (1992), Zepeda (1998), Petrizzo (2000, 2003), Campbell et al. (2004), Petrizzo et al. (2011) and Thibault et al. (2012). Magnetostratigraphy is after Galbrun (1992) and

113 Thibault et al. (2012). See supplementary material for further information and Supplementary
114 material Table 1.

115 Foraminiferal preservation was evaluated to be poor (P) for specimens that show minor
116 test fragmentation, are overgrown with secondary calcite, and show cement infilling (Fig. 2, 1a–
117 d). Foraminifera judged as having moderate (M) preservation are slightly overgrown with
118 secondary calcite, or show some cement infilling with minor signs of test fragmentation (Fig. 2,
119 2a–c and 3a–c). A good (G) preservation rating is given for foraminifera whose tests are
120 recrystallized but do not exhibit calcite overgrowths, cement infillings, or fragmentation and
121 whose tests are not translucent under the light microscope, (Fig. 2, 4a–c). Foraminiferal
122 preservation was evaluated to be very good (VG) when signs of recrystallization were not
123 discernible in transmitted light and test walls were almost optically translucent (Fig. 2, 5a–b, 6a–
124 c and 7a–b) (see Supplementary material Table 2). The shells of specimens with good to very
125 good preservation have been slightly altered by diagenetic processes, but high magnification
126 SEM images of wall microstructure (Fig. 2, 7b) reveal the presence of smooth walls and open
127 pores that indicate primary calcite and increase the probability that primary trends are preserved
128 (Pearson et al., 2001).

129 At Hole 762C, foraminiferal preservation is generally poor to moderate in the
130 Cenomanian, moderate to very good in the Turonian–Coniacian and good to very good from the
131 Santonian to the Maastrichtian. The best-preserved specimens within each sample were selected
132 for stable-isotope ratio analyses (see Supplementary Material Table 2 for preservation of
133 specimens measured). No glassy foraminifera, planktonic or benthic, were found throughout the
134 stratigraphic interval examined. To characterize broad-scale stratigraphic changes in
135 foraminiferal preservation more fully, elemental abundances were measured for mixed

planktonic and benthic foraminiferal samples throughout the examined stratigraphic interval (see Supplementary material Fig. 1 and Supplementary material Table 3).

Stable-isotope analyses presented here are based on 1 to 8 planktonic foraminiferal specimens depending on their test size. To obtain species-specific $\delta^{18}O$ and $\delta^{13}C$ values, we processed 1 to 3 large-sized keeled to partially keeled trochospiral specimens (*Rotalipora*, *Helvetoglobotruncana, Falsotruncana*, *Praeglobotruncana, Dicarinella*, *Marginotruncana*, *Contusotruncana*, *Globotruncana*, *Globotruncanita*, and *Abathomphalus* spp.), 2 to 5 medium-sized trochospiral (*Whiteinella*, *Archaeoglobigerina*, *Costellagerina*, and *Rugoglobigerina* spp.) and serial (*Pseudotextularia*, *Racemiguembelina* spp.) specimens, and 4 to 8 specimens of the remaining genera ("*Heterohelix*", *Gublerina*, *Globigerinelloides*, and *Muricohedbergella* spp.). Results obtained for each species were used to calculate the maximum, minimum and average $\delta^{18}O$ and $\delta^{13}C$ values of each genus in the samples examined (Fig. 3). Because benthic foraminifera at Site 762C are rare, usually infilled with carbonate cement and relatively small-sized, the number of specimens available for processing was not sufficient to obtain species-specific stable-isotope analyses. Consequently, benthic results are based on analyses of 2 to 3 specimens of different species belonging to the genera *Lenticulina*, *Gyroidinoides*, *Gavelinella*, and *Colomia*.

Most foraminiferal stable-isotope ratio data were generated using a Thermo Finnegan™ Delta Plus dual-inlet IRMS with Kiel III on-line automated carbonate reaction system at the University of Missouri. Data are expressed as per mil values on the Vienna PDB (VPDB) scale, after normalization based on the difference between the within-run average measured and recommended values ($\delta^{13}C$ = -1.95‰, $\delta^{18}O$ = -2.20‰) for NBS-19. Replicate measurements of NBS-19 yielded an external precision of ±0.028‰ for $\delta^{13}C$ and ±0.055‰ for $\delta^{18}O$ values,

159 respectively, (1 σ, n=157) of the uncorrected values for the standards. Stable-isotope ratios of
160 <63 μm fine fractions and other foraminiferal samples were generated at the University of
161 Oxford using a VG PRISM IRMS and common acid-bath preparation system (Clarke and
162 Jenkyns, 1999; Clarke, 2002). Data are expressed as per mil values on the Vienna PDB scale,
163 after normalization based on the difference between the within-run average accepted values for
164 an internal laboratory Carrara marble standard that had been calibrated against NBS-19. The
165 external precision for the Oxford dataset is better than 0.1‰ for both $\delta^{13}C$ and $\delta^{18}O$ values.
166
167 **RESULTS**
168 Oxygen stable-isotope ratios ($\delta^{18}O$ values) range from -0.5 to -3.0‰ for the <63 μm fine
169 fraction, from 0.5 to -2.5‰ for benthic foraminifera, and from -1.0‰ to -4.5 for planktonic
170 foraminifera, with a consistent intra-sample range of ~1.5‰ among co-occurring planktonic
171 foraminiferal genera (Fig. 3). In general, the oxygen-isotope trend shown by benthic specimens
172 follows the trend of planktonic foraminifera, and the gradient between planktonic and benthic
173 foraminifera ranges from ~1.5‰ in the Turonian–Coniacian interval and ~0.5‰ in the
174 Maastrichtian. The Cenomanian–mid-Santonian foraminiferal record shows relatively constant
175 $\delta^{18}O$ values for each taxon, followed by an increase of ~1‰ from the mid-Santonian through the
176 mid-Campanian among all groups. The upper Campanian–Maastrichtian is characterized by
177 short-term $\delta^{18}O$ fluctuations of ~1‰, implying more variable climatic conditions, but no long-
178 term directional climate change.
179 The $\delta^{18}O$ values of the <63 μm fine fraction mainly fall in between the $\delta^{18}O$ values
180 displayed by planktonic and benthic foraminifera and generally follows planktonic foraminiferal
181 trends. Fine-fraction results show relatively high variability throughout the Cenomanian–lower

Santonian and during the upper Campanian–Maastrichtian and relatively low variability during the remaining time intervals.

Carbon stable-isotope ratios ($\delta^{13}C$ values) range from ~1.0 to 3.5‰ for the <63 μm fine fraction, from 0.5 to 2.5‰ for benthic foraminifera and from 1.0 to 3.0‰ for planktonic foraminifera, with a slightly increasing range of values among co-occurring planktonic foraminiferal genera from 0.5‰ in the Cenomanian–Turonian to >1.0‰ during the Maastrichtian (Fig. 3). Following a ~2‰ rise through the Cenomanian–early Turonian and a peak in the mid-Turonian–lower Santonian, the average $\delta^{13}C$ values displayed by planktonic and benthic foraminifera remain stable at ~2.7‰ and ~1.5‰, respectively, from the upper Turonian through the upper Campanian. The uppermost Campanian–Maastrichtian interval is characterized by low-amplitude fluctuations followed by a decrease close to the Cretaceous/Paleogene (K/Pg) boundary, in line with global trends (Voigt et al., 2012).

The $\delta^{13}C$ values for the <63 μm fine fraction follow very closely the highest values exhibited by planktonic foraminifera in any sample; that is, fine fraction and planktonic foraminiferal trends are very similar. In addition, the fine-fraction curve exhibits short-term high-amplitude fluctuations at the base (Cenomanian–lower Santonian) and at the top of the sequence (upper Campanian–Maastrichtian), but displays constant values through the remaining stratigraphic interval.

More negative $\delta^{13}C$ values, <1.0‰ and even <0.0‰, are evident within the deepest Hole 762C hemipelagic carbonate sediments (Supplementary Figure 2), with these attributed to diagenetic alteration, as described below and in the supplementary information.

DISCUSSION

205 **Long-term trends in $\delta^{18}O$ and $\delta^{13}C$ values**

206 The absence of glassy foraminiferal tests indicates that $\delta^{18}O$ values are unlikely to be
207 entirely primary and hence estimates of past seawater temperatures might be compromised by a
208 diagenetic component. Clarke and Jenkyns (1999) also demonstrated that the Hole 762C fine
209 fraction record registered lower $\delta^{18}O$ values than coeval stratigraphic intervals from the
210 shallower buried sediments recovered in Exmouth Plateau Holes 763B and 766A. Nevertheless,
211 the observed quality of preservation among specimens analyzed suggests that, with the exception
212 of the deepest Cenomanian and oldest Turonian intervals, foraminiferal tests within Hole 762C
213 preserve long-term trends in $\delta^{18}O$ and $\delta^{13}C$ values. In addition and most importantly, it is evident
214 that offsets in stable-isotope ratios among sample types, including between different planktonic
215 foraminiferal species are preserved (Pearson et al., 2001; Sexton et al., 2006), a condition
216 essential for reconstruction of long-term climatic trends and interpretations of paleoecological
217 preferences of fossil taxa (Boersma and Shackleton, 1981 and many subsequent studies).
218 Reliability of the majority of stable-isotope results is further supported by foraminiferal
219 elemental data (see Supplementary material).

220 Despite there being a general consensus that maximum mid-Cretaceous greenhouse
221 warmth occurred during the Cenomanian–Turonian, available compilations of benthic
222 foraminiferal and brachiopod $\delta^{18}O$ data indicate that maximum temperatures were reached
223 during the late Cenomanian (Huber et al., 1999; Voigt et al., 2004; Cramer et al., 2009; Friedrich
224 et al., 2012), while certain bulk and foraminiferal $\delta^{18}O$ records (Clarke and Jenkyns, 1999;
225 Wilson et al., 2002; Jarvis et al., 2011) show peak warmth within the early Turonian. Such a
226 discrepancy in the apparent timing of maximum warmth might have been caused by: (a) poor
227 biostratigraphic control in depth–age model development and/or weak correlation between sites,

228 (b) localized micro-recrystallization within the foraminiferal tests that might have biased
229 temporal paleotemperature estimates and/or (c) local/regional oceanographic signals that differ in
230 detail from global trends. The Hole 762C planktonic foraminiferal $\delta^{18}O$ record obtained during
231 this study indicates a ~8 myr-long (Turonian–mid-Santonian; 93–85 Ma) surface-ocean "warm
232 plateau" an observation consistent with TEX_{86} paleothermometry of equatorial Atlantic
233 sediments (Demerara Rise: Forster et al., 2007; Bornemann et al., 2008), as well as with $\delta^{18}O$
234 values for well-preserved planktonic foraminifera from the southern tropical to high latitudes
235 (Falkland Plateau, Naturaliste Plateau and Maud Rise: Huber et al., 1995, 2002; Tanzania:
236 MacLeod et al., 2013). On the other hand, the fine-fraction $\delta^{18}O$ record at Site 762C indicates
237 more unstable conditions with differences between adjacent samples of up to 1.0 to 1.5‰. The
238 mid-Santonian–mid-Campanian cooling trend, followed by shorter term late Campanian–
239 Maastrichtian warming and cooling episodes indicated by planktonic foraminifera, benthic
240 foraminifera and fine-fraction data (Fig. 3) corresponds closely to coeval trends elsewhere based
241 on $\delta^{18}O$ values on foraminifera (Li and Keller, 1999; Friedrich et al., 2012; Ando et al., 2013)
242 and TEX_{86} paleothermometry (Linnert et al., 2014).
243 The long-term foraminiferal and fine-fraction $\delta^{13}C$ profile at Exmouth Plateau (Fig. 3)
244 records a series of major positive and negative excursions (~1‰) in the Turonian–Coniacian
245 interval. The $\delta^{13}C$ positive shift culminating in the lowermost Turonian might be interpreted as
246 the typical excursion across the Cenomanian/Turonian boundary (corresponding to the Oceanic
247 Anoxic Event 2: Jenkyns et al., 1994; Jarvis et al., 2006, among others), especially given the
248 occurrence of dark shales in this stratigraphic interval (Haq et al., 1990). However, available
249 $\delta^{13}C$ data from below the studied interval (820 to ~835 mbsf) indicate that at Hole 762C a trend
250 to higher $\delta^{13}C$ values begins at about 835 mbsf around the base of the hemipelagic carbonates,

(See Supplementary Fig. 2) in an interval comprised between the upper Albian and the mid-Cenomanian (Bralower and Siesser, 1992; Wonders, 1992), at least 2 myr before the globally recorded C/T boundary isotopic anomaly. Therefore, the positive trend in $\delta^{13}C$ values observed at the base of the studied interval, increasing from $\delta^{13}C$ values <1‰ for fine-fraction samples and <0‰ for planktonic and benthic foraminifera (which also have similar absolute $\delta^{13}C$ values between ~805 and ~835 mbsf) most likely results from diagenetic alteration that overprinted the original isotopic signal (see Supplementary Figure 2). The Hole 762C Cenomanian hemipelagic carbonate-containing sediments are unconformably underlain by Lower Cretaceous deltaic sediments containing organic carbon (TOC content up to 2%: Haq et al., 1990). It seems that upward migration of ^{12}C-enriched pore fluids from these deltaic sediments has compromised the Cenomanian (and possibly the earliest Turonian) carbonate $\delta^{13}C$ record, most likely during early diagenesis. A diagenetic interpretation is supported by the clear downhole trend to progressively lower fine-fraction and foraminiferal $\delta^{13}C$ values below ~805 mbsf, by the relatively high degree of recrystallization seen within the Cenomanian interval, and by the elemental data that are most clearly manifested by the stepped increases in bulk foraminiferal Mg and Mn concentrations below ~810 mbsf (see Supplementary Material for detailed discussion).

The most obvious consequence of diagenetic alteration of the Cenomanian and lowermost Turonian carbonates is removal of the expected C/T boundary positive $\delta^{13}C$ excursion, although the $\delta^{18}O$ values below ~805–810 mbsf also could be considered suspect if the pore fluids originating from the deltaic sediments had a unique $\delta^{18}O$ composition (see Supplementary Material for detailed discussion). It is further evident from the variability in the $\delta^{13}C$ records above ~805–810 mbsf that the influence of the ^{12}C-enriched pore fluids was restricted primarily to the Cenomanian and lowermost Turonian stratigraphic interval. We cannot

exclude the possibility that the $\delta^{13}C$ negative excursion registered in the lowermost Turonian (top of core 74X) might represent the recovery phase after the typical C/T positive anomaly, as it falls in an interval where the isotopic signal seems to be less diagenetically altered, but given apparent alteration in subjacent samples, we do not argue that this shift is primary.

A lower amplitude (~0.5‰) positive excursion of planktonic foraminifera and fine-fraction $\delta^{13}C$ values is observable in the mid–late Maastrichtian within magnetic chron C30N (core 45X) and stratigraphically corresponds to the "Exmouth Plateau Event" identified at Hole 762C by Thibault et al. (2012) based on the $\delta^{13}C$ bulk isotopic curve. The "Exmouth Plateau Event" has been detected by Thibault et al. (2012) in the benthic foraminiferal $\delta^{13}C$ record available for ODP Hole 761B drilled at the Exmouth Plateau (Barrera and Savin, 1999), and in the $\delta^{13}C$ bulk curve available for ODP Hole 1210B (Shatsky Rise, equatorial Pacific Ocean) and for sections from Northern Germany in Voigt et al. (2012), whereas it corresponds to a minor (0.1‰) positive $\delta^{13}C$ shift in the Umbria–Marche Basin (Thibault et al., 2012). Because of the limited extent or absence of isotopic excursions in several localities, the "Exmouth Plateau Event" was interpreted as a regional phenomenon by Thibault et al. (2012). The two-step rise of the $\delta^{13}C$ bulk curve associated with the mid-Maastrichtian event (MME), recognized by Voigt et al. (2012) and Wendler (2013) in several localities across latitudes (Umbria–Marche Basin, Northern Germany, Denmark, DSDP Site 525: Walvis Ridge, South Atlantic Ocean, ODP Hole 690C: Maud Rise, Southern Ocean and ODP Hole 1210B: Shatsky Rise), falls in a younger stratigraphic interval within magnetic chron C31N and apparently is absent at Hole 762C, because it falls within the Maastrichtian hiatus (Thibault et al., 2012).

It is worth noting, however, that mid-Maastrichtian environmental perturbations related to changes in the source region of intermediate and/or deep-water masses were originally

297 postulated by MacLeod (1994) and MacLeod and Huber (1996) and invoked as a possible cause
298 for the extinction among inoceramids, which is found to be diachronous across latitudes
299 (MacLeod et al., 1996; Nifuku et al., 2009). However, in all sites examined by MacLeod and
300 Huber (1996), the extinction of inoceramids is preceded by a negative excursion of benthic
301 foraminiferal $\delta^{13}C$ values falling within magnetic chron C31R (where magnetostratigraphic data
302 are available). Frank and Arthur (1999) compared late Campanian–Maastrichtian benthic
303 foraminiferal $\delta^{13}C$ values from Pacific, Atlantic and Southern Ocean sites and distinguished three
304 time intervals of alternating large and small inter-ocean offsets, which have been related to
305 changes in deep-sea circulation. In detail, the second time interval (upper part of C31R to the top
306 of C31N) characterized by the lowest inter-ocean $\delta^{13}C$ gradient was interpreted as the time of
307 global homogenization of intermediate and deep waters that may have caused the extinction
308 among inoceramids.
309 In summary, the environmental perturbations that have been related to the MME are
310 exemplified by different isotopic signals within different chronostratigraphic intervals, as
311 follows: 1) two-step rise of the $\delta^{13}C$ bulk curve within magnetic chron C31N, 2) negative $\delta^{13}C$
312 benthic foraminiferal excursions falling within magnetic chron C31R, and 3) a reduced inter-
313 ocean benthic foraminifera $\delta^{13}C$ gradient identified from the upper part of C31R to the top of
314 C31N. Consequently, caution has to be paid when using MME-related isotopic shifts for global
315 correlation.
316 Concerning long-term variations in the structure of the water-column, the Hole 762C
317 record indicates a ~0.5‰ increase in the $\delta^{13}C$ offset among planktonic foraminiferal genera from
318 the early Maastrichtian compared to the underlying stratigraphic interval. Interestingly, an early–
319 mid-Maastrichtian increase in the $\delta^{13}C$ offset between foraminifera has been also detected in the

central Atlantic (Blake Nose, ODP Site 1050C: Isaza-Londoño et al., 2006), in the South Atlantic (Walvis Ridge, DSDP Hole 525A: Abramovich et al., 2003) and central Pacific (Shatsky Rise, DSDP Site 577A: Abramovich et al., 2003) Oceans, suggesting possible global variations (i.e., increased sea-surface stratification and/or establishment of a deeper nutricline) in the structure of the water column, and/or evolution of species with new life strategies, including the possible acquisition of photosymbionts. A photosymbiotic habit was likely adopted by only few lineages during the mid-Campanian (Abramovich et al., 2003; Falzoni et al., 2013, 2014), but it might have represented a progressively more common life strategy during the Maastrichtian, paralleling the evolution and diversification of biserial and multiserial taxa and of other surface-dwellers (D'Hondt and Zachos, 1998; Houston et al., 1999; Isaza-Londoño et al., 2006).

Reliability of <63 µm fine-fraction stable-isotopes for tracing long-term Cretaceous $\delta^{18}O$ and $\delta^{13}C$ trends

The <63 µm size fraction is the coccolith-rich component of a pelagic sediment and surface-ocean plankton assemblage, but in several Hole 762C stratigraphic intervals this size fraction also includes small and rare juvenile planktonic and benthic foraminifera and pithonellids (Fig. 4a–d). The $\delta^{18}O$ and $\delta^{13}C$ isotopic signal of polyspecific nannofossil assemblages has been used as a proxy to trace Miocene (Ennyu et al., 2002: Rio Grande Rise, DSDP Site 516; Lord Howe Rise, DSP Site 588; King's Trough, DSDP Site 608) and mid-Cretaceous (Ando et al., 2010: Blake Nose, ODP Site 1050C) surface-ocean properties, because oxygen- and carbon-isotope trends were found to be similar to those shown by co-occurring planktonic and benthic foraminifera.

However, studies on living coccolithophorid algae have documented a very large and variable (from 1 to 5‰: Dudley et al., 1986; Ziveri et al., 2003) species-specific offset in $\delta^{18}O$ and $\delta^{13}C$ values between coccolith calcite and ambient seawater due to vital effects. Therefore, recent studies (Ziveri et al., 2003; Candelier et al., 2013) have suggested using the fine-fraction isotopic signal only if based on monospecific coccoliths with well-constrained vital effects, but offsets attributed to vital effects are manifestly difficult to know accurately for fossil species. Moreover, other recent studies have suggested that Cenozoic coccolithophore vital effects are an adaptation to decreasing atmospheric carbon dioxide concentrations that developed after the Paleocene–Eocene Thermal Maximum (Stoll et al., 2002; Bolton et al., 2012; Bolton and Stoll, 2013). Consequently, the array of coccolithophorid vital effects might have been different (or even absent) during the high pCO_2 mid- to Late Cretaceous world, further complicating interpretation of the isotopic values yielded by the Hole 762C coccolith-rich fraction.

Comparison of the Exmouth Plateau record with the long-term stable-isotope ratios of paired fossil foraminifera and coccolithophorid algae available in the literature (Miocene: Ennyu et al., 2002; mid-Cretaceous: Ando et al., 2010) illustrates similarities and discrepancies as follows: 1) coccolithophore algae are expected to inhabit a very shallow ocean surface layer, because they are photosynthetic organisms; however, the fine-fraction $\delta^{18}O$ values are higher than those shown by planktonic foraminifera and always fall in between the values exhibited by planktonic and benthic species (see also benthic foraminiferal $\delta^{18}O$ values for Hole 1050C in Petrizzo et al., 2008); 2) at Hole 762C, the $\delta^{18}O$ fine-fraction trend is punctuated by high-amplitude fluctuations (1.0 to 1.5‰) that do not always mirror foraminiferal trends. This feature is peculiar to Hole 762C and not reported in other published studies, despite the stratigraphic resolution of the foraminiferal record being identical or even higher than the fine-fraction record

365 when both records are available; 3) at Hole 762C, the fine-fraction $\delta^{13}C$ values parallel
366 planktonic foraminiferal trends, but are generally higher, whereas the fine-fraction $\delta^{13}C$ curves of
367 Ennyu et al. (2002) and Ando et al. (2010) fall close to the average values yielded by planktonic
368 foraminifera.

369 Fine-fraction $\delta^{18}O$ values falling in between the values exhibited by planktonic and
370 benthic species are found in all the records available, and most importantly also at Blake Nose
371 (northwest Atlantic Ocean) where foraminiferal specimens are exceptionally well preserved
372 ("quasi-glassy" in some intervals: Ando et al., 2010). Assuming that glassy-textured foraminifera
373 preserve a good estimate of the $\delta^{18}O$ of ambient sea-water (Pearson et al., 2001) and that
374 foraminiferal vital effects more significantly affect $\delta^{13}C$ rather than $\delta^{18}O$ values (Pearson, 1998),
375 $\delta^{18}O$ values yielded by the fine-fraction might have been originally higher than those shown by
376 planktonic foraminifera at the Exmouth Plateau (i.e., the difference could be primary not a
377 diagenetic artifact), as at the Blake Nose. Therefore, relatively high fine-fraction $\delta^{18}O$ values
378 could be explained in part by disequilibrium during secretion of coccolithophorid calcite from
379 ambient seawater, because the average offset between the $\delta^{18}O$ displayed by the fine fraction and
380 planktonic foraminifera (1 to 2‰) falls within the range of variability of the vital effects
381 calculated for living coccolithophorid algae (1 to 5‰). That said, a higher susceptibility to
382 alteration at or near the seafloor for the fine fraction compared to individual foraminiferal tests
383 alone could explain the offset between their $\delta^{18}O$ values, and sample-to-sample differences in the
384 diagenetic overprint could explain the presence of high-amplitude fluctuations in the
385 Cenomanian–lower Santonian and lower Maastrichtian fine-fraction isotopic data (Fig. 2,
386 Supplementary material Fig. 1 and Supplementary material Table 3), whereas younger and more
387 shallowly buried material (mid-Santonian–Maastrichtian) is generally better preserved. Although

388 large-sized foraminifera that showed calcite infillings, or apparent signs of recrystallization after
389 examination under the light microscope, were excluded from isotopic analyses, the diagenetic
390 alteration of the <63 μm size-fraction was not discernable under the light microscope. The upper
391 Campanian–Maastrichtian $\delta^{18}O$ fine-fraction fluctuations are almost in phase with foraminifera
392 and are likely not related to diagenesis as foraminiferal preservation and elemental data analyses
393 (see Supplementary material Fig. 1) do not indicate major alteration. Therefore, fine-fraction
394 $\delta^{18}O$ values might have preserved the original signal and most probably represent the response of
395 coccolithophorid algae to the late Campanian–Maastrichtian warming–cooling episodes.
396 However, $\delta^{18}O$ fine-fraction fluctuations in the interval from 620 to 600 mbsf are not in phase
397 with the $\delta^{18}O$ foraminiferal trends and show a rather high offset from the $\delta^{18}O$ values of the
398 underlying and overlying samples, suggesting that some diagenetic alteration might have
399 overprinted the original isotopic signal. Finally, reasons for explaining the unusually high fine-
400 fraction $\delta^{13}C$ values compared to planktonic foraminifera are not discernible based on the
401 available data, but are possibly related to local conditions of the nutricline or seasonal production
402 of coccoliths or other photoautotrophs during times of maximum sea-surface $^{13}C/^{12}C$ ratio,
403 possibly after the bulk of the nutrients had been exhausted and seasonal stratification was
404 established.

405 The present study suggests that while long-term carbon-isotope ratio trends derived from
406 the <63 μm fine fraction are likely reliable as tracers of surface ocean $^{13}C/^{12}C$ ratios, problems in
407 evaluating the preservation of coccoliths in the fine fraction, as well as the unknown (potential)
408 vital effects of Cretaceous nannofossil species might complicate the interpretation of long-term
409 oxygen-isotope trends, if not supported by other proxies.
410

411 **Planktonic Foraminiferal Depth Habitats and Species Turnover**

412 The isotope records from Hole 762C span a major 3-myr time interval with an associated
413 turnover among Late Cretaceous planktonic foraminifera. This worldwide change in the
414 planktonic foraminiferal assemblages (i.e., Hart, 1999; Premoli Silva and Sliter, 1999) includes
415 extinction of several forms, including *Falsotruncana*, bi-convex *Dicarinella* species (*D. hagni*,
416 *D. imbricata* and *D. canaliculata*), weakly keeled *Praeglobotruncana*, and globigeriniform
417 *Whiteinella*, as well as radiation of the double-keeled *Marginotruncana*. During the
418 Coniacian–Santonian transition there were first appearances of several keeled genera, including
419 *Contusotruncana*, *Globotruncana*, *Globotruncanita*, umbilico-convex *Dicarinella* species (i.e.,
420 *D. concavata* and *D. asymetrica*), and globigeriniform taxa within the genera *Costellagerina* and
421 *Archaeoglobigerina* (Fig. 3). This Coniacian–Santonian phase was followed by the extinction of
422 the pre-Campanian, keeled genera (*Marginotruncana* and *Dicarinella*) and by the proliferation of
423 *Globotruncana*, *Globotruncanita* and *Contusotruncana* across another 3-myr interval (latest
424 Santonian–early Campanian, Premoli Silva and Sliter, 1999).

425 The causes for this faunal replacement have been linked to changes in surface- and deep-
426 water circulation and to the Late Cretaceous cooling trend that might have modified surface-
427 ocean habitats (Premoli Silva and Sliter, 1999; Petrizzo, 2002). Accordingly, recent studies based
428 on neodymium isotope ratios confirm that the early Campanian was a time of re-organization of
429 intermediate and deep-sea circulation patterns at a global scale (Robinson et al., 2010; MacLeod
430 et al., 2011; Murphy and Thomas, 2012; Robinson and Vance, 2012). Interestingly, the Late
431 Cretaceous Nd-isotope ratio composite record from Hole 762C (<1000 m paleodepth; Voigt et
432 al., 2013) and Hole 763B (~1000 m paleodepth; Murphy and Thomas, 2012) show some
433 correlations with the long-term planktonic foraminiferal $\delta^{18}O$ trends reported here. The Nd-

434 isotopic values of these shallower sites show values and trends similar to the deeper bathyal
435 Exmouth Plateau Site 765 (~3000 m paleodepth) and Argo Abyssal Plain Site 766 (~4000 m
436 paleodepth) (see Robinson et al., 2010; Murphy and Thomas, 2012) suggesting that both were
437 bathed by the same water mass (Murphy and Thomas, 2012). At Hole 763B, Nd-isotopic values
438 are relatively high (~ -7‰) during the Turonian–early Campanian but shift to distinctly lower
439 values (~ -11‰) from the early–mid-Campanian throughout the Maastrichtian. The early–mid-
440 Campanian shift has been interpreted as an expansion of intermediate and deep waters sourced in
441 southern mid–high latitudes during the Campanian–Maastrichtian cooling (Robinson et al., 2010;
442 Murphy and Thomas, 2012; Robinson and Vance, 2012). The planktonic foraminiferal $\delta^{18}O$
443 record reported here indicates that the onset of cooling (mid-Santonian) in the Indian Ocean
444 preceded the Nd-isotopic shift at bathyal depths on Exmouth Plateau. This result does not mean
445 Campanian–Maastrichtian climate changes and circulation patterns were not linked (e.g.,
446 Robinson et al., 2010; MacLeod et al., 2011; Robinson and Vance, 2012), but it does illustrate
447 the importance of considering evidence of local to regional conditions as well as global trends in
448 explaining Nd-isotopic shifts.
449 In terms of the planktonic foraminiferal assemblages, turnover occurred during an
450 interval of relatively stable Nd isotopic values (Turonian–Santonian) suggesting that variations
451 in the intermediate and deep-ocean circulation did not directly cause the observed
452 extinctions/radiations. Instead, planktonic foraminiferal turnover mainly involved large-sized
453 keeled species (diameter > 300 μm and up to 700 μm) with similar morphologies considered to
454 have comparable paleoecological preferences (e.g., Caron and Homewood 1983; Premoli Silva
455 and Sliter, 1999; Hart, 1999), such that extinction and radiation of different taxa thought to have

456 occupied the same habitat has been difficult to explain using the traditional paleoecology (i.e.,
457 depth habitat) model based on test morphology.

458 Hole 762C stable-isotope ratio data further support several recent studies on glassy-
459 textured foraminifera (Petrizzo et al., 2008; Ando et al., 2010; Falzoni et al., 2013) that found a
460 number of exceptions to the morphology-based assignment of species-specific depth habitats.
461 Whilst several keeled taxa (i.e., *Falsotruncana* and bi-convex *Dicarinella* species) were
462 effectively deeper/cool dwellers, as recognized by the morphology model and supported by the
463 isotope ratio data presented here, many double-keeled species, for which few or no isotope ratio
464 data were previously available in the literature (umbilico-convex *Dicarinella*, most
465 *Marginotruncana* and *Contusotruncana* species) yield an isotopic signature that suggests a
466 shallower/warmer water-column habitat. Particularly evident in the present dataset is the depth
467 distribution of the umbilico-convex *Dicarinella* and of the *Marginotruncana* species that
468 inhabited a shallow ecological niche, despite their double-keeled periphery, large test size and
469 their complex morphology, whereas taxa that co-occur in the same late Coniacian–Santonian
470 interval and possess similar morphological features (*Globotruncana*, *Globotruncanita* and
471 *Contusotruncana*) show an isotopic signature indicative of a deeper/colder habitat.

472 In the light of these new findings, we suggest that the late Coniacian–early Santonian
473 turnover occurred over a 3-myr period when *Marginotruncana* specimens progressively
474 occupied all of the ecological niches available. This habitat invasion was likely possible because
475 *Marginotruncana* species were more easily able to adapt to a wider temperature/salinity range
476 (as inferred from their $\delta^{18}O$ values). This hypothesized successful adaptation is also supported by
477 the increase in *Marginotruncana* species diversity from their appearance during the Turonian, in
478 parallel with the decrease in species diversity of those taxa experiencing extinction (Petrizzo,

2002). Thus, this major turnover was likely due to the competition exerted by the more generalist *Marginotruncana* over the more selective *Falsotruncana*, bi-convex *Dicarinella* and *Praeglobotruncana*. It is worth noting that the order of planktonic foraminiferal extinction mirrors their depth ranking in the water column from the deepest (*Falsotruncana*) to the shallowest dwellers (*Whiteinella*).

Marginotruncana and *Dicarinella* extinctions are clearly correlated with the onset of the Santonian–Campanian cooling combined with likely competition exerted by *Globotruncana*, *Contusotruncana* and *Globotruncanita* within particular depth habitats. The latter genera initially diverged from their keeled shallow-dwelling marginotruncanid ancestors to occupy a deeper/colder habitat and subsequently migrated upward in the water column as their ancestors disappeared and surface-ocean temperatures decreased. We infer that the onset of significant cooling during the mid-Santonian led to the expansion of the deep/cold ecological niches that favored the proliferation of globotruncanids and negatively affected all shallow-dwelling taxa that had evolved during hotter greenhouse times. Further support for this interpretation is provided by the delayed extinction of *Marginotruncana* species in the tropical Tethyan Realm (e.g., at the top of the *G. elevata* Zone in the Bottaccione section: Premoli Silva and Sliter, 1995; Coccioni and Premoli Silva, 2015) when compared with mid-latitude localities (in the lowermost *G. elevata* Zone at the Exmouth Plateau: Petrizzo, 2000). Moreover, the timing of species extinctions, first the shallowest dwelling umbilico-convex *Dicarinella* species, and later the slightly deeper dwelling *Marginotruncana* species, parallels specific steps of surface ocean cooling and further supports the conclusions presented here (Fig. 3).

CONCLUSIONS

In agreement with other studies from the southern high latitudes, the new planktonic foraminiferal $\delta^{18}O$ record from Exmouth Plateau indicates extreme greenhouse conditions persisting from the early Turonian to the mid-Santonian, a prolonged cooling from the mid Santonian to the mid-Campanian and short-term warming-cooling episodes during the late Campanian–Maastrichtian. This study also confirms that foraminiferal $\delta^{18}O$ data represent an accurate tool for tracing relative changes in bottom- and surface-ocean temperatures, because specimens used for isotopic analyses can be preferentially selected based on visual assessment of their preservation. On the other hand, the influence of isotopic vital effects for Cretaceous calcareous nannofossils remains currently unknown. These findings potentially have implications for the reliability of bulk-carbonate isotope trends without additional supporting data such as benthic or planktonic foraminiferal oxygen-isotope ratios.

Moreover, we suggest that the main Coniacian turnover among planktonic foraminifera was caused by evolution of a new temperature/salinity-tolerant genus (*Marginotruncana*), whereas the extinction of *Dicarinella* and *Marginotruncana* was correlated to the onset of surface-ocean cooling during the mid-Santonian and to competition with deeper dwellers in cooler waters (globotruncanids). Because the timing and patterns of the turnover among planktonic foraminiferal assemblages are similar throughout the mid–low latitudes, we infer that the combination of the biotic and abiotic forces identified at the Exmouth Plateau likely drove planktonic foraminiferal evolution at a global scale. Finally, this study represents a substantial contribution toward the understanding of Earth climate dynamics during the Late Cretaceous and provides new insights into the relationship between climate change and planktonic foraminiferal evolution during hot to mild greenhouse climate phases.

ACKNOWLEDGMENTS

This manuscript has benefited from the useful comments provided by the Science Editor David Ian Schofield, Associate Editor Thomas Olszewski and referee R. Mark Leckie. We are greatly indebted to Elisabetta Erba for thoughtful discussions on the interpretation of the fine-fraction isotopic signal. This study was supported by the Cushman Foundation for Foraminiferal Research (Johanna M. Resig Fellowship 2011 to FF), which is warmly acknowledged. FF and MRP were partially funded through MIUR (Italian Ministry of University and Research) PRIN grant 2010–2011 (2010X3PP8J_001) to E. Erba and PUR 2008 (University of Milan). LJC was supported by a NERC DPhil studentship award when at the University of Oxford. Agostino Rizzi (CNR, Italy) is thanked for assistance at the SEM and Shannon Haynes for work on stable-isotope ratio analyses at the University of Missouri. The Ocean Drilling Program is acknowledged for making available the samples for this study.

REFERENCES CITED

Abramovich, S., Keller, G., Stüben, D., and Berner, Z., 2003, Characterization of late Campanian and Maastrichtian planktonic foraminiferal depth habitats and vital activities based on stable isotopes: Palaeogeography, Palaeoclimatology, Palaeoecology, v. 202, p. 1–29, doi: 10.1016/S0031-0182(03)00572-8.

Abramovich, S., Yovel-Corem, S., Almogi-Labin, A., and Benjamini, C., 2010, Global climate change and planktic foraminiferal response in the Maastrichtian: Paleoceanography, v. 25, PA2201, doi: 10.1029/2009PA001843.

547 Ando, A., Huber, B.T., and MacLeod, K.G., 2010, Depth-habitat reorganization of planktonic
548 foraminifera across the Albian/Cenomanian boundary: Paleobiology, v. 36, p. 357–373, doi:
549 10.1666/09027.1.
550 Ando, A., Woodard, S.C., Evans, H.F., Littler, K., Herrmann, S., MacLeod, K.G., Kim, S.,
551 Khim, B.-K., Robinson, S.A., and Huber, B.T., 2013, An emerging palaeoceanographic
552 'missing link': Multidisciplinary study of rarely recovered parts of deep-sea Santonian–
553 Campanian transition from Shatsky Rise: Journal of the Geologic Society of London, v. 170,
554 p. 381–384, doi:10.1144/jgs2012-137.
555 Barrera, E., and Savin, S.M., 1999, Evolution of late Campanian–Maastrichtian marine climates
556 and oceans, *in* Barrera, E., Johnson, C.C., eds., The Evolution of the Cretaceous Ocean-
557 Climate System: Boulder, Colorado, Geological Society of America Special Paper, v. 332, p.
558 245–282.
559 Bice, K.L., Birgel, D., Meyers, P.A., Dahl, K.A., Hinrichs, K.-U., and Norris, R.D., 2006, A
560 multiple proxy and model study of Cretaceous upper ocean temperatures and atmospheric
561 CO_2 concentrations: Paleoceanography, v. 21, PA2002, doi: 10.1029/2005PA001203.
562 Boersma, A., and Shackleton, N.J., 1981, Oxygen- and carbon-isotope variations and
563 planktonic-foraminifer depth habitats, Late Cretaceous to Paleocene, Central Pacific, Deep
564 Sea Drilling Project Sites 463 and 465, *in* Thiede, J., Vallier, T. L., et al., eds., Initial
565 Reports of the Deep Sea Drilling Project: U.S. Government Printing Office, Washington,
566 D.C., v. 62, p. 355–360.
567 Bolton, C.T., Stoll, H.M., and Mendez-Vicente, A., 2012, Vital effects in coccolith calcite:
568 Cenozoic climate-pCO_2 drove the diversity of carbon acquisition strategies in
569 coccolithophores?: Paleoceanography, v. 27, PA4204, doi:10.1029/2012PA002339.

570 Bolton, C.T., and Stoll, H.M., 2013, Late Miocene threshold response to marine algae to carbon
571 dioxide limitation: Nature, v. 500, p. 558–562, doi:10.1038/nature12448.
572 Bornemann, A., Norris, R.D., Friedrich, O., Beckmann, B., Schouten, S., Sinninghe Damsté
573 J.S., Vogel, J., Hofmann, P., and Wagner, T., 2008, Isotopic evidence for glaciation during
574 the Cretaceous Supergreenhouse: Science, v. 319, p. 189–192, doi:
575 10.1126/science.1148777.
576 Bralower, T.J., and Siesser, W.G., 1992, Cretaceous calcareous nannofossil biostratigraphy of
577 Sites 761, 762, and 763, Exmouth and Wombat Plateaus, northwestern Australia, *in* von
578 Rad, U., Haq, B.U., et al., eds., Proceedings of the Ocean Drilling Program, Scientific
579 Results: College Station, TX (Ocean Drilling Program), v. 122, p. 529–556.
580 Campbell, R.J., Howe, R.W., and Rexilius, J.P., 2004, Middle Campanian–lowermost
581 Maastrichtian nannofossil and foraminiferal biostratigraphy of the northwestern Australian
582 margin: Cretaceous Research, v. 25, p. 827–864. doi: 10.1016/j.cretres.2004.08.003.
583 Candelier, Y., Minoletti, F., Probert, I., and Hermoso, M., 2013, Temperature dependence of
584 oxygen isotope fractionation in coccoliths calcite: a culture and core top calibration of the
585 genus *Calcidiscus*: Geochimica et Cosmochimica Acta, v. 100, p. 264–281, doi:
586 10.1016/j.gca.2012.09.040.
587 Caron, M., and Homewood, P., 1983, Evolution of early planktic foraminifers: Marine
588 Micropaleontology, v. 7, p. 453–462, doi: 10.1016/0377-8398(83)90010-5.
589 Clarke, L.J., and Jenkyns, H.C., 1999, New oxygen isotope evidence for long-term Cretaceous
590 climatic change in the Southern Hemisphere: Geology, v. 27, p. 699–702, doi:
591 10.1130/0091-7613(1999)027<0699:NOIEFL>2.3.CO;2.

592 Clarke, L.J., 2002, Stable-isotopic evidence for long-term mid- to Late Cretaceous climatic and
593 oceanographic change, DPhil thesis, University of Oxford, U.K.
594 Coccioni, R., and Premoli Silva, I., 2015, Revised Upper Albian–Maastrichtian planktonic
595 foraminiferal biostratigraphy and magneto-stratigraphy of the classical Tethyan Gubbio
596 section (Italy): Newsletters on Stratigraphy, v. 48, p. 47–90.
597 Cramer, B.S., Toggweiler, J.R., Wright, J.D., and Katz, M.E., 2009, Ocean overturning since
598 the Late Cretaceous: inferences from a new benthic foraminiferal isotope compilation:
599 Paleoceanography, v. 24, PA4216, doi: 10.1029/2008PA001683.
600 D'Hondt, S., and Zachos, J.C., 1998, Cretaceous foraminifera and the evolutionary history of
601 planktic photosymbiosis: Paleobiology, v. 24, p. 512–523.
602 Dudley W.C., Blackwelder P., Brand L. and Duplessy J.-C., 1986, Stable isotopic composition
603 of coccoliths: Marine Micropaleontology, v. 10, p. 1–8.
604 Ennyu, A., Arthur, M.A., and Pagani, M., 2002, Fine-fraction carbonate stable isotopes as
605 indicators of seasonal shallow mixed-layer paleohydrography: Marine Micropaleontology, v.
606 46, p. 317–342, doi: 10.1016/S0377-8398(02)00079-8.
607 Falzoni, F., and Petrizzo, M.R., 2011, Taxonomic overview and evolutionary history of
608 *Globotruncanita insignis* (Gandolfi, 1955): Journal of Foraminiferal Research, v. 41, p. 371–
609 383, doi: 10.2113/gsjfr.41.4.371.
610 Falzoni, F., Petrizzo, M.R., MacLeod, K.G., and Huber, B.T., 2013, Santonian–Campanian
611 planktonic foraminifera from Tanzania, Shatsky Rise and Exmouth Plateau: species depth
612 ecology and paleoceanographic inferences: Marine Micropaleontology, v. 103, p. 15–29,
613 doi: 10.1016/0377-8398(83)90010-5.

614 Falzoni, F., Petrizzo, M.R., Huber, B.T., and MacLeod, K.G., 2014, Insights into the
615 meridional ornamentation of the planktonic foraminiferal genus *Rugoglobigerina* (Late
616 Cretaceous) and implications for taxonomy: Cretaceous Research, v. 47, p. 87–104, doi:
617 10.1016/j.cretres.2013.11.001.
618 Falzoni, F., Petrizzo, M.R., Jenkyns, H.C, Gale, A.S., and Tsikos, H., 2016, Planktonic
619 foraminiferal biostratigraphy and assemblage composition across the Cenomanian–Turonian
620 boundary interval at Clot Chevalier (Vocontian Basin, SE France): Cretaceous Research, v.
621 59, p. 69–97, doi: 10.1016/j.cretres.2015.10.028.
622 Forster, A., Schouten, S., Baas, M., and Sinninghe Damsté, J.S., 2007, Mid-Cretaceous
623 (Albian–Santonian) sea surface temperature record of the tropical Atlantic Ocean: Geology,
624 v. 35, p. 919–922, doi: 10.1130/G23874A.
625 Frank, T.D., and Arthur, M.A., 1999, Tectonic forcings of Maastrichtian ocean-climate
626 evolution: Paleoceanography, v. 14, p. 103–117, doi: 10.1029/1998PA900017.
627 Friedrich, O., Norris, R.D., and Erbacher, J., 2012, Evolution of middle to Late Cretaceous
628 oceans–A 55 m.y. record of Earth's temperature and carbon cycle: Geology, v. 40, p. 107–
629 110, doi: 10.1130/G32701.1.
630 Galbrun B., 1992, Magnetostratigraphy of upper Cretaceous and lower Tertiary sediments, sites
631 761 and 762, Exmouth Plateau, northwest Australia, *in* von Rad, U., Haq, B.U., et al., eds.,
632 Proceedings of the Ocean Drilling Program, Scientific Results: College Station, TX (Ocean
633 Drilling Program), v. 122, p. 699–716.
634 Haq, B.U., von Rad, U., O'Connell, S., et al., 1990, Proceedings of the Ocean Drilling
635 Program, Initial Reports, Volume 122: College Station, TX (Ocean Drilling Program).

636 Hart, M.B., 1999, The evolution and biodiversity of Cretaceous Foraminiferida: Geobios, v. 32,
637 no. 2, p. 247–255.
638 Hay, W.W., DeConto, R., Wold, C.N., Wilson, K.M., Voigt, S., Schulz, M., Wold-Rossby, A.,
639 Dullo, W.C., Ronov, A.B., Balukhovsky, A.N., and Soeding, E., 1999, Alternative global
640 Cretaceous paleogeography, in Barrera, E., Johnson, C.C., eds., The evolution of the
641 Cretaceous ocean/climate system: Boulder, Colorado, Geological Society of America
642 Special Paper, v. 332, p. 1–47.
643 Haynes, S.J., Huber, B.T., and Macleod, K.G., 2015, Evolution and phylogeny of mid-
644 Cretaceous (Albian–Coniacian) biserial planktic foraminifera: Journal of Foraminiferal
645 Research, v. 45, p. 42–81.
646 Houston, R.M., Huber, B.T., and Spero, H.J., 1999, Size-related isotopic trends in some
647 Maastrichtian planktic foraminifera: methodological comparisons, intraspecific variability,
648 and evidence for photosymbiosis: Marine Micropaleontology, v. 36, p. 169–188, doi:
649 10.1016/S0377-8398(99)00007-9.
650 Huber, B.T., Hodell, D.A., and Hamilton, C.P., 1995, Middle-Late Cretaceous climate of the
651 southern high latitudes: Stable isotopic evidence for minimal equator-to-pole thermal
652 gradients: Geological Society of America Bulletin, v. 107, p. 1164–1191, doi:
653 10.1130/0016-7606(1995)107<1164:MLCCOT>2.3.CO;2.
654 Huber, B.T., Leckie, R.M., Norris, R.D., Bralower, T.J., and CoBabe, E., 1999, Foraminiferal
655 assemblage and stable isotopic change across the Cenomanian-Turonian boundary in the
656 subtropical North Atlantic: Journal of Foraminiferal Research, v. 29, p. 392–417.

Huber, B.T., Norris, R.D., and MacLeod, K.G., 2002, Deep-sea paleotemperature record of extreme warmth during the Cretaceous: Geology, v. 30, p. 123–126, doi: 10.1130/0091-7613(2002)030<0123:DSPROE>2.0.CO;2.

Huber, B.T., and Leckie, R.M., 2011, Planktic foraminiferal species turnover across deep-sea Aptian/Albian boundary sections: Journal of Foraminiferal Research, v. 41, p. 53–95, doi: 10.2113/gsjfr.41.1.53.

Isaza-Londoño, C., MacLeod, K.G., and Huber, B.T., 2006, Maastrichtian North Atlantic warming, increasing stratification, and foraminiferal paleobiology at three timescales: Paleoceanography, v. 21, PA1012, doi: 10.1029/2004PA001130.

Jarvis, I., Gale, A.S., Jenkyns, H.C., and Pearce, M.A., 2006, Secular variation in Late Cretaceous carbon isotopes: a new $\delta^{13}C$ carbonate reference curve for the Cenomanian–Campanian (99.6–70.6 Ma): Geological Magazine, v. 143, p. 561–608, doi: 10.1017/S0016756806002421.

Jarvis, I., Lignum, J.S., Gröcke, D.R., Jenkyns, H.C., and Pearce, M.A., 2011, Black shale deposition, atmospheric CO_2 drawdown, and cooling during the Cenomanian- Turonian Oceanic Anoxic Event: Paleoceanography, v. 26, PA3201, doi: 10.1029/2010PA002081.

Jenkyns, H.C., Gale, A.S., and Corfield, R.M., 1994, Carbon- and oxygen-isotope stratigraphy of the English Chalk and Italian Scaglia and its palaeoclimatic significance: Geological Magazine, v. 131, p. 1–34.

Li, L., and Keller, G., 1999, Variability in Late Cretaceous climate and deep waters: evidence from stable isotopes: Marine Geology, v. 161, p. 171–190, doi:10.1016/S0025-3227(99)00078-X.

679 Linnert, C., Robinson, S.A., Lees, J.A., Bown, P.N., Pérez-Rodríguez, I., Petrizzo, M.R.,
680 Falzoni, F., Littler, K., Arz, J.A., and Russell, E.E., 2014, Evidence for global cooling in the
681 Late Cretaceous: Nature Communications, v. 5, no. 4194, doi: 10.1038/ncomms5194.
682 Loeblich, A.R.Jr., and Tappan, H., 1987, Foraminiferal Genera and their Classification: Van
683 Nostrand Rienhold Company, New York, 2 vol., 970 pp.
684 MacLeod, K.G., 1994, Bioturbation, inoceramid extinction, and mid-Maastrichtian ecological
685 change: Geology, v. 22, p. 139–142, doi: 10.1130/0091-7613(1994)022<0139:BIEAMM>
686 2.3.CO;2.
687 MacLeod, K.G., and Huber, B.T., 1996, Reorganization of deep ocean circulation
688 accompanying a Late Cretaceous extinction event: Nature, v. 380, p. 422–425, doi:
689 10.1038/380422a0.
690 MacLeod, K.G., Huber, B.T., and Ward, P.D., 1996, The biostratigraphy and paleobiology of
691 Maastrichtian inoceramids, *in* Ryder, G., et al., eds., The Cretaceous-Tertiary event and
692 other catastrophes in Earth history: Geological Society of America Special Paper, v. 307, p.
693 361–373.
694 MacLeod, K.G., Huber, B.T., and Isaza Londoño, C., 2005, North Atlantic warming during
695 global cooling at the end of the Cretaceous: Geology, v. 33, p. 437–440, doi:
696 10.1130/G21466.1.
697 MacLeod, K.G., Isaza Londoño, C., Martin, E.E., Jiménez Berrocoso, Á., and Basak, C., 2011,
698 Nd evidence for changes in North Atlantic Circulation at the end of the Cretaceous
699 greenhouse: Nature Geoscience, v. 4, p. 779–782, doi: 10.1038/ngeo1284.

MacLeod, K.G., Huber, B.T., Jiménez Berrocoso, Á., and Wendler, I., 2013, A stable and hot Turonian without glacial $\delta^{18}O$ excursions is indicated by exquisitely preserved Tanzanian foraminifera: Geology, v. 41, no. 10, p. 1083–1086, doi: 10.1130/G34510.1.

Moriya, K., Wilson, P.A., Friedrich, O., Erbacher, J., and Kawahata, H., 2007, Testing for ice sheets during the mid-Cretaceous greenhouse using glassy foraminiferal calcite from the mid-Cenomanian tropics on Demerara Rise: Geology, v. 35, p. 615–618; doi: 10.1130/G23589A.1.

Murphy, D.P., and Thomas, D.J., 2012, Cretaceous deep-water formation in the Indian sector of the Southern Ocean: Paleoceanography, v. 27, PA1211, doi: 10.1029/2011PA002198.

Nifuku, K., Kodama, K., Shigeta, Y., and Naruse, H., 2009, Faunal turnover at the end of the Cretaceous in the North Pacific region: Implications from combined magnetostratigraphy and biostratigraphy of the Maastrichtian Senpohshi Formation in the eastern Hokkaido Island, northern Japan: Palaeogeography, Palaeoclimatology, Palaeoecology, v. 271, p. 84–95, doi: 10.1016/j.palaeo.2008.09.012.

Pearson, P.N., 1998, Stable isotopes and the study of evolution in planktonic foraminifera, The Paleontological Society Papers, v. 4, p. 138–178.

Pearson, P.N., Ditchfield, P.W., Singano, J.M., Harcourt-Brown, K.G., Nicholas, C.J., Olsson, R.K., Shackleton, N.J., and Hall, M.A., 2001, Warm tropical sea surface temperatures in the Late Cretaceous and Eocene epochs: Nature, v. 413, p. 481–487, doi: 10.1038/35097000.

Petrizzo, M.R., 2000, Upper Turonian-lower Campanian planktonic foraminifera from southern mid-high latitudes (Exmouth Plateau, NW Australia): biostratigraphy and taxonomic notes: Cretaceous Research, v. 21, p. 479–505, doi: 10.1006/cres.2000.0218.

722 Petrizzo, M.R., 2002, Palaeoceanographic and palaeoclimatic inferences from Late Cretaceous
723 planktonic foraminiferal assemblages from the Exmouth Plateau (ODP Sites 762 and 763,
724 eastern Indian Ocean): Marine Micropaleontology, v. 45, p. 117–150, doi: 10.1016/S0377-
725 8398(02)00020-8.
726 Petrizzo, M.R., 2003, Late Cretaceous planktonic foraminiferal bioevents in the Tethys and in
727 the Southern Ocean record: an overview: Journal of Foraminiferal Research, v. 33, p. 330–
728 337, doi: 10.2113/0330330.
729 Petrizzo, M.R., Huber, B.T., Wilson, P.A., and MacLeod, K.G., 2008, Late Albian
730 paleoceanography of the western subtropical North Atlantic: Paleoceanography, v. 23,
731 PA1213, doi: 10.1029/2007PA001517.
732 Petrizzo, M.R., Falzoni, F., and Premoli Silva, I., 2011, Identification of the base of the lower-
733 to-middle Campanian *Globotruncana ventricosa* Zone: comments on reliability and global
734 correlations: Cretaceous Research, v. 32, p. 387–405, doi: 10.1016/j.cretres.2011.01.010.
735 Petrizzo, M. R., Caron, M., and Premoli Silva, I., 2015, Remarks on the identification of the
736 Albian/Cenomanian boundary and taxonomic clarification of the planktonic foraminifera
737 index species *globotruncanoides*, *brotzeni* and *tehamaensis*: Geological Magazine, v. 152, p.
738 521–536, doi: 10.1017/S0016756814000478.
739 Premoli Silva, I., and Sliter, W.V., 1995, Cretaceous planktonic foraminiferal biostratigraphy
740 and evolutionary trends from the Bottaccione section, Gubbio, Italy: Palaeontographia
741 Italica, v. 81, p. 2–90.
742 Premoli Silva, I., and Sliter, W.V., 1999, Cretaceous paleoceanography: evidence from
743 planktonic foraminiferal evolution, *in* Barrera, E., Johnson, C.C., eds., The Evolution of the

744 Cretaceous Ocean-Climate System: Boulder, Colorado, Geological Society of America
745 Special Paper, v. 332, p. 301–328, doi: 10.1130/0-8137-2332-9.301.
746 Robaszynski, F., Caron, M., and the European Working Group on Planktonic Foraminifera,
747 1979, Atlas of mid Cretaceous planktonic foraminifera (Boreal Sea and Tethys), C.N.R.S.
748 Paris, France: Cahiers de Micropaléontologie, v. 1 and 2.
749 Robaszynski, F., Caron, M., Gonzalez-Donoso, J.M., Wonders, A.H., and the European
750 Working Group on Planktonic Foraminifera, 1984, Atlas of Late Cretaceous
751 Globotruncanids: Revue de Micropaléontologie, v. 26, p. 145–305.
752 Robinson, S.A., Murphy, D.P., Vance, D., and Thomas, D.J., 2010, Formation of "Southern
753 Component Water" in the Late Cretaceous: Evidence from Nd-isotopes: Geology, v. 38, p.
754 871–874, doi: 10.1130/G31165.1.
755 Robinson, S.A., and Vance, D., 2012, Widespread and synchronous change in deep-ocean
756 circulation in the North and South Atlantic during the Late Cretaceous: Paleoceanography,
757 v. 27, PA1102, doi: 10.1029/2011PA002240.
758 Sexton, P.F., Wilson, P.A., and Pearson, P.N., 2006, Microstructural and geochemical
759 perspectives on planktonic foraminiferal preservation: "glassy" versus "frosty":
760 Geochemistry, Geophysics, Geosystems, v. 7, p. 1–29, doi: 10.1029/2006GC001291.
761 Sinninghe Damsté, J.S., Kuypers, M.M.M., Pancost, R.D., and Schouten, S., 2008, The carbon
762 isotopic response of algae, (cyano)bacteria, archaea and higher plants to the late
763 Cenomanian perturbation of the global carbon cycle: Insights from biomarkers in black
764 shales from the Cape Verde Basin (DSDP Site 367): Organic Geochemistry, v. 39, p. 1703–
765 1718, doi:10.1016/j.orggeochem.2008.01.012.

766 Stoll, H.M., Klaas, C.M., Probert, I., Encinar, J.R., and Alonso, J.I.G., 2002, Calcification rate
767 and temperature effects on Sr partitioning in coccoliths of multiple species of
768 coccolithophorids in culture: Global and Planetary Change, v. 34, p. 153–171.
769 Thibault, N., Husson, D., Harlou, R., Gardin, G., Galbrun, B., Huret, E., and Minoletti, F.,
770 2012, Astronomical calibration of upper Campanian–Maastrichtian carbon isotope events
771 and calcareous plankton biostratigraphy in the Indian Ocean (ODP Hole 762C): Implication
772 for the age of the Campanian–Maastrichtian boundary: Palaeogeography,
773 Palaeoclimatology, Palaeoecology, v. 337–338, p. 52–71, doi:
774 10.1016/j.palaeo.2012.03.027.
775 Voigt, S., Gale, A.S., and Flögel, S., 2004, Midlatitude shelf seas in the Cenomanian-Turonian
776 greenhouse world: temperature evolution and North Atlantic circulation: Paleoceanography,
777 v. 19, PA4020, doi: 10.1029/2004PA001015.
778 Voigt, S., Gale, A.S., Jung, C., and Jenkyns, H.C., 2012, Global correlation of Upper
779 Campanian–Maastrichtian successions using carbon-isotope stratigraphy: development of a
780 new Maastrichtian timescale: Newsletters on Stratigraphy, v. 45, p. 25–53, doi:
781 10.1127/0078-0421/2012/0016.
782 Voigt, S., Jung, C., Friedrich, O., Frank, M., Teschner, C., and Hoffmann, J., 2013,
783 Tectonically restricted deep-ocean circulation at the end of the Cretaceous greenhouse: Earth
784 and Planetary Science Letters, v. 369-370, p. 169–177, doi: 10.1016/j.epsl.2013.03.019.
785 Wendler, I., 2013, A critical evaluation of carbon isotope stratigraphy and biostratigraphic
786 implications for Late Cretaceous global correlation: Earth-Science Reviews, v. 126, p. 116–
787 146, doi: 10.1016/j.earscirev.2013.08.003.

Wilson, P.A., Norris, R.D., and Cooper, M.J., 2002, Testing the Cretaceous greenhouse hypothesis using glassy foraminiferal calcite from the core of the Turonian tropics on Demerara Rise: Geology, v. 30, p. 607–610. doi: 10.1130/0091-7613(2002)030<0607:TTCGHU>2.0.CO;2.

Wonders, A.A.H., 1992, Cretaceous planktonic foraminiferal biostratigraphy, Leg 122, Exmouth Plateau, Australia, *in* von Rad, U., Haq, B.U., et al., eds., Proceedings of the Ocean Drilling Program, Scientific Results: College Station, TX (Ocean Drilling Program), v. 122, p. 587–599.

Zepeda, M.A., 1998, Planktonic foraminiferal diversity, equitability and biostratigraphy of the uppermost Campanian–Maastrichtian, ODP Leg 122, Hole 762C, Exmouth Plateau, NW Australia, eastern Indian Ocean: Cretaceous Research, v. 19, p. 117–152, doi: 10.1006/cres.1997.0097.

Ziveri P., Stoll H., Probert I., Klaas C., Geisen M., Ganssen G., and Young J., 2003, Stable isotope vital effects in coccolith calcite: Earth and Planetary Science Letters, v. 210, p. 137–149, doi: 10.1016/S0012-821X(03)00101-8.

FIGURE CAPTIONS

Figure 1. Paleogeographic reconstruction for the mid-Campanian (80 Ma), with location and paleolatitude of Exmouth Plateau (ODP Hole 762C). After Hay et al. (1999).

Figure 2. SEM images of planktonic and benthic foraminiferal specimens showing differential preservation. Poor Preservation: 1a–d) *Praeglobotruncana* sp., sample 762C-71X-2, 51–53 cm (Coniacian). Moderate preservation: 2a–c) *Lenticulina* sp., sample 762C-66X-4, 80–82 cm (Santonian); 3a–c) *Globotruncana linneiana*, sample 762C-66X-5, 58–60 cm (Santonian).

Good preservation: 4a–c) *Marginotruncana angusticarenata*, sample 762C-66X-2, 66–68 cm (Santonian). Very good preservation: 5a–b) "*Heterohelix"* sp., sample 762C-59X-1, 140–142 cm (Campanian); 6a–c) *Muricohedbergella flandrini*, sample 762C-66X-3, 7–9 cm (Santonian); 7a–b) *Rugoglobigerina pennyi*, sample 762C-54X-1, 12–14 cm (Campanian). Scale bar = 100 μm unless differently specified.

Figure 3. Exmouth Plateau (Hole 762C) foraminiferal and fine-fraction (<63 μm) carbon- and oxygen-isotope ratios plotted against stratigraphy. Colored symbols of planktonic foraminifera indicate average values; bars indicate maximum and minimum values, when replicate measurements are available. Lithostratigraphy after Haq et al. (1990), planktonic foraminiferal biostratigraphy after Haq et al., (1990), Zepeda (1998), Petrizzo (2000), Campbell (2004), Petrizzo et al. (2011); calcareous nannofossil biostratigraphy after Bralower and Siesser (1992) and Thibault et al. (2012); magnetostratigraphy after Galbrun (1992). Oxygen-isotope ratio values of the fine-fraction curve are from Clarke and Jenkyns (1999). Species grouped under the name *Dicarinella* plano-convex include *D. hagni*, *D. imbricata* and *D. canaliculata*. Abbreviations–Ages: Cen = Cenomanian; Planktonic foraminiferal biozones: *c. = Rotalipora cushmani*, *arch = Whiteinella archaeocretacea*, *helv. = Helvetoglobotruncana helvetica*, *maslakov. = Falsotruncana maslakovae*, *mar. = Marginotruncana marianosi*.

Figure 4. SEM images of the fine fraction (< 63 μm) from Hole 762C: a) coccolith plates and fragments of coccolith elements, sample 762C-44X-3, 60–62, scale bar = 10 μm; b) a biserial planktonic foraminiferal specimen and few coccoliths, sample 762C-59X-2, 45–47, scale bar = 50 μm; c) a preserved coccosphere with coccoliths, sample 762C-59X-2, 45–47, scale bar = 10 μm; d) a calcisphere and coccoliths, sample 762C-59X-2, 45–47, scale bar = 50 μm.

Figure 1

Click here to download Figure Falzoni et al., Fig. 1.pdf

Falzoni et al., Figure 1, pdf

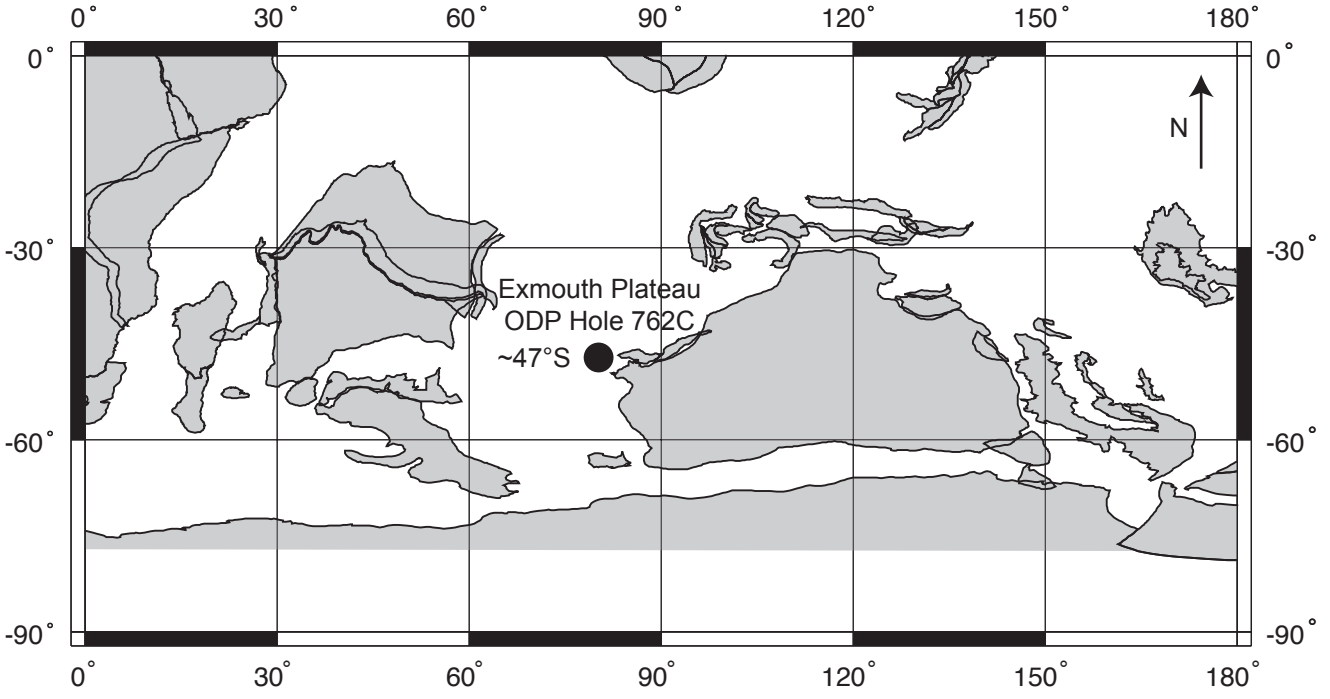

Click here to download Figure Falzoni et al., Fig 2.pdf

Falzoni et al., Figure 2, pdf

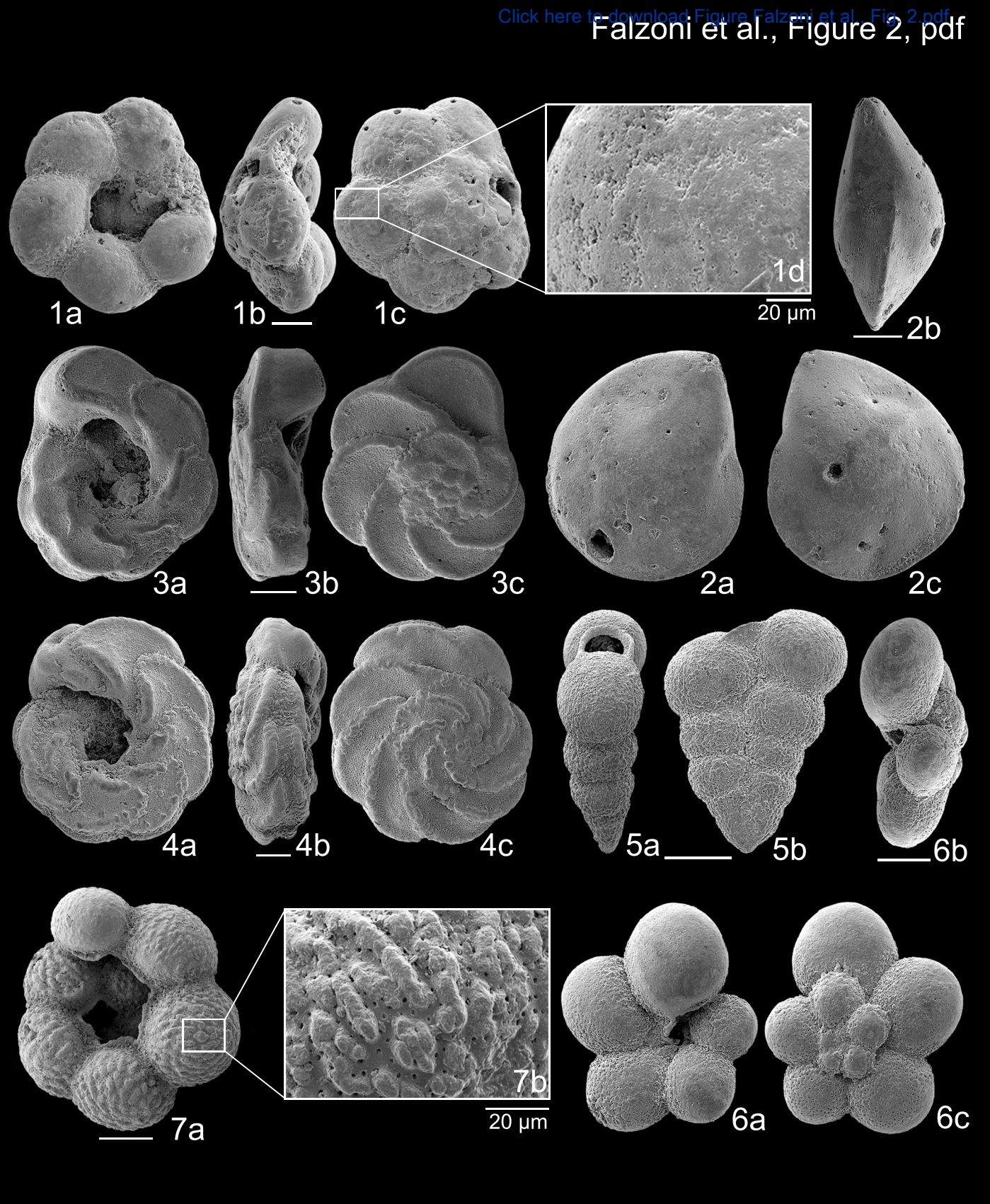

Click here to download Figure Fig. 3-ox-carb trends.pdf

Exmouth Plateau - Hole 762C

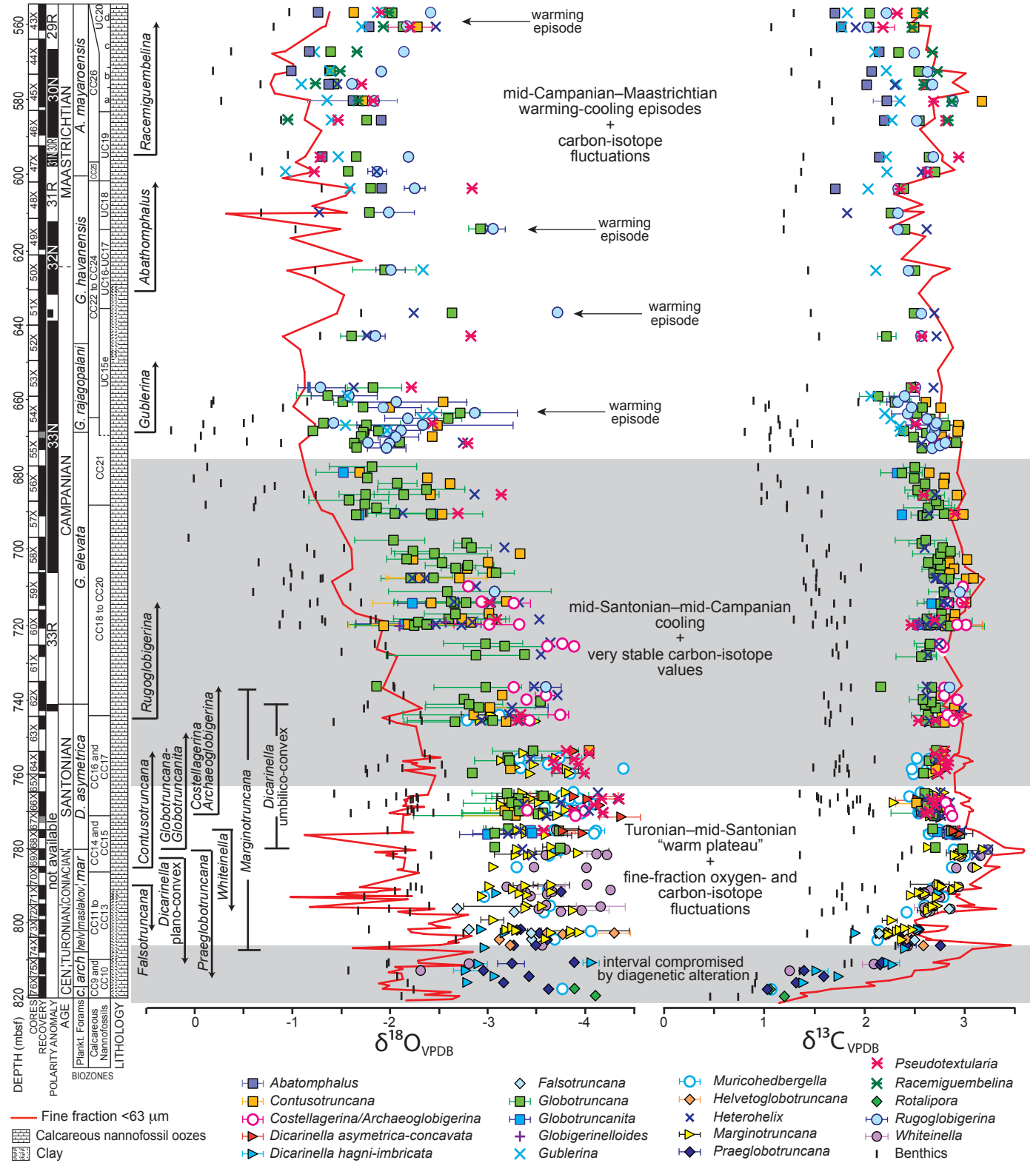

Click here to download Figure Falzoni et al. Fig. 4.pdf

Falzoni et al., Figure 4, pdf